



A co-evolutionary lane-changing trajectory planning method for automated vehicles based on the instantaneous risk identification

Jiabin Wu^a, Xiaohua Chen^b, Yiming Bie^{c,*}, Wei Zhou^d

^a School of Transportation, Civil Engineering & Architecture, Foshan University, Foshan 528225, China

^b School of Civil Engineering and Transportation, South China University of Technology, Guangzhou 510641, China

^c School of Transportation, Jilin University, Changchun 130022, China

^d Department of Civil & Environmental Engineering, National University of Singapore, 117576, Singapore



ARTICLE INFO

Keywords:

Traffic engineering
Intelligent vehicle
Lane change planning
Risk identification

ABSTRACT

Lane-changing trajectory planning (LTP) is an effective concept to control automated vehicles (AVs) in mixed traffic, which can reduce traffic conflicts and improve overall traffic efficiency. To enhance the lane change safety for AVs, a co-evolutionary lane-changing trajectory planning (CLTP) method is proposed to describe the risk minimization process that co-evolves with the dynamic traffic environment in the limited literature. Firstly, the natural driving data of vehicle trajectory on the expressway provided by the High dataset are used to construct the lane-changing samples. To obtain the future traffic environment information, a deep learning neural network is adopted to capture trajectory dynamics in mobility of surrounding vehicles around a lane-changing vehicle. Secondly, the safe interaction between the subject vehicle and the surrounding vehicles is considered to establish a mathematical model for the temporal and spatial risk identification of a lane change event based on the fault tree analysis method. Subsequently, the risk minimization of lane change is considered as the objective. Based on the acceleration and deceleration overtaking rules and the trapezoidal acceleration method, the longitudinal and lateral displacement schemes during a lane change are designed. Finally, the motion parameters of longitudinal and lateral displacement are acquired to form an ideal lane change trajectory using a genetic algorithm. The results show that this method can effectively achieve higher safety of the lane-changing process, and reduce the traffic conflicts and traffic turbulence caused by dangerous lane-changing behaviors. The findings can provide theoretical support for lane change trajectory planning algorithm design of intelligent vehicles.

1. Introduction

Lane change is one of the most common driving behaviors. The previous study has shown that traffic accidents caused by lane changes account for 5 % of the total number of accidents, of which 75 % are caused by driver's decision-making mistakes (Yang et al., 2017; Lim et al., 2021). Some researchers aimed to develop automatic driving technology or lane change assistance system to improve lane-changing safety and reduce the collision risk caused by wrong decisions made by drivers through automatic lane change or early warning (Huang et al., 2019; Xu et al., 2018). To decrease the serious traffic conflicts during a lane change, this study mainly focuses on the lane-changing trajectory planning (LTP) algorithm in automatic driving systems. Compared with the car-following behavior, the subject vehicle (SV)

needs to consider the lateral and longitudinal control of the vehicle during the lane-changing process, which involves the interaction with surrounding vehicles, conflict resolution, track feasibility, comfort and stability. However, the researches on lane-changing trajectory planning of AVs are more challenging and require further development.

Lane change is a complex maneuver and its safety is usually affected by surrounding vehicles in multiple lanes (Chen et al., 2021; Zhai and Wu, 2022). In a lane change, the SV will gradually move from the gap between the front vehicle (FV) and the rear vehicle (RV) on the current lane to the gap between the preceding vehicle (PV) and the lag vehicle (LV) on the target lane. One can see that the motion states of FV, RV, PV and LV have a significant impact on the lane-changing safety of the SV. Existing studies on LTP usually assumed that all surrounding vehicles around the SV maintained a constant speed, and only one lane-changing trajectory corresponding to the initial states of surrounding vehicles was

* Corresponding author.

E-mail address: yimingbie@126.com (Y. Bie).

Nomenclature	
SV	Subject vehicle
FV	Front vehicle in the current lane
RV	Rear vehicle in the current lane
PV	Preceding vehicle in the target lane
LV	Lag vehicle in the target lane
x_j	The x-coordinate for the boundary line of column j
y_i	The y-coordinate for the boundary line of row i
S	Maximum longitudinal detection distances of SV
E	Maximum lateral detection distances of SV
$Cell(x_{ij}^k, y_{ij}^k)$	Cell coordinate of vehicle k is column j in row i
x_t^k	Coordinate of surrounding vehicle k at time t
r	Reset gate
z	Update gate
h	Current memory content
s_t^k	Final memory of surrounding vehicle k at the current time step
σ	Sigmoid activation function
x_t^k	Observed data of surrounding vehicle k at time t
U^i	Update transfer matrix
W^i	Weight matrix
$s_{t t+k}^0$	The positions of SV at the predicted time $t t+k$
$s_{t t+k}^i$	The positions of surrounding vehicle i at the predicted time $t t+k$
$SDI_i(t t+k)$	Stopping distance index between the SV and surrounding vehicle i at the predicted time $t t+k$
$D_F(t t+k)$	Stopping sight distance of the vehicle in the forward position between the SV and surrounding vehicle i at the predicted time $t t+k$
$D_R(t t+k)$	SSD of the vehicle in the rear position between SV and surrounding vehicle i at the predicted time $t t+k$
$D_j(t t+k)$	SSD of the vehicle j (including the SV and surrounding vehicles, $j=0$ represents the SV) at the predicted time $t t+k$
$d_i(t)$	Longitudinal distance between the SV and surrounding vehicle i at the predicted time $t t+k$
l_F	Length of the vehicle that stays at the forward position
f	Surface friction coefficient
t_r	Driver perception time
g	Road grade
$\varphi_s(t t+k)$	Instantaneous risk coefficient of the SV at the predicted time $t t+k$
$\eta_i(t t+k)$	Failure event possibility of safe interaction between the SV and surrounding vehicle i ($i=1, \dots, n, n \leq 4$) at the predicted time $t t+k$
$TRL_i(t t+k)$	Temporal risk level between the SV and surrounding vehicle i ($i=1, \dots, n$) at the predicted time $t t+k$
$SRL_i(t t+k)$	Spatial risk level between the SV and surrounding vehicle i ($i=1, \dots, n$) at the predicted time $t t+k$
TTC_i	Time to the collision between the SV and surrounding vehicles i ($i=1, \dots, n$)
MTC_i	Margin to the collision between the SV and surrounding vehicles i ($i=1, \dots, n$)
TIT_i	Time-integrated time to the collision between the SV and surrounding vehicles i ($i=1, \dots, n$)
$SDI_i^{cri}(t t+k)$	Theoretical maximum SDI at the predicted time $t t+k$
σ	The sum of the average action time of drivers and the effective time of the vehicle braking system
$x_s^{start}(t_s)$	Longitudinal position when the SV starts to change lanes
t_s	The beginning time of lane change for the SV
t_c	Lane change duration
$x_s^{end}(t_s + t_c)$	Longitudinal position of the SV at the end of the lane change
x_i	Longitudinal position of the surrounding vehicle i , $i=1, 2, 3, 4$
a_y^{max}	Maximum lateral acceleration of the SV
k_a	The change rate of lateral acceleration of the SV
t	Time variable at the future moment
$f(t)$	Unit step function. t_1, t_2, t_3 and t_4 are transient time variables
t_1	The starting instants when the SV reaches the maximum lateral acceleration
t_2	The ending instants when the SV reaches the maximum lateral acceleration
t_3	The starting instants when the SV reaches the minimum lateral acceleration
t_4	The ending instants when the SV reaches the minimum lateral acceleration
D	Horizontal spacing between the center lines of the two lanes
$g(t+\tau)$	Lane-changing risk of the SV at the predicted time $t+\tau$
n	Number of surrounding vehicles ($n \leq 4$)
M_1	The penalty coefficients of temporal risk between SV and surrounding vehicles at the predicted time $t+\tau$
M_2	The penalty coefficients of spatial risk between the SV and surrounding vehicles at the predicted time $t+\tau$
τ	Any moment within the lane change duration t_c
δ_1	Safe thresholds of temporal risks
δ_2	Safe thresholds of spatial risks
$V_S(t+\tau)$	The longitudinal speed of SV at the predicted time $t+\tau$
V_L	Maximum longitudinal speed limit of SV
$a_x(t+\tau)$	Longitudinal acceleration of SV at the predicted time $t+\tau$
a_L	Maximum longitudinal acceleration of SV under the premise of driving comfort

planned. However, the speed of surrounding vehicles tends to vary over time randomly. The SV needs to consider the movement of surrounding vehicles and dynamically adjust its speed and acceleration to maintain the safety distances from the FV, RV, PV and LV. Therefore, a new trajectory should be designed for each time unit based on real-time data of surrounding vehicles. With the rapid development of sensors and communication technologies, the real-time information of surrounding vehicles can be accurately captured. The theoretical research on dynamic lane-changing trajectory planning (DLTP) has emerged and its application has gradually become possible.

However, the existing studies on the DLTP models are few so far. Luo et al. (2016) proposed a DLTP model by capturing the real-time information of surrounding vehicles through connected vehicle technology. The model failed to consider the reaction time of the system and

assumed that the initial acceleration of SV was zero, which was inconsistent with the actual situation. Yang et al. (2018) established a new DLTP model by designing the modules of the starting point determination, trajectory decision and trajectory generation. The model evades the unrealistic assumptions of lane-changing speed and acceleration, and further ensures the lane-changing safety of automatic vehicles. However, the existing DLTP models still have some limitations. Firstly, the models only consider the interactive impact of the PV and LV on the target lane in terms of lane-changing safety. However, before the SV completely crosses the lane line, its safety will also be disturbed by the motion states of the FV and RV on the original lane (Ali et al., 2021). Secondly, most studies adjust the lane-changing trajectory based on the current motion information of the surrounding vehicles in each time step. As a result, the associated LTP process may have a significant time

lag, and the predictability of the future motion information of the surrounding vehicles tends to be ignored. Finally, few studies have considered the temporal and spatial risks of AVs and the adjustment strategy of longitudinal position before a lane change, which can achieve better safety and smoothness in the lane-changing process.

Although the existing studies have achieved encouraging results, the further development is needed. To address the limitations of the existing models, a novel co-evolutionary lane-changing trajectory planning (CLTP) model based on the future motion information of surrounding vehicles is proposed. Compared with previous researches, this study has the following advantages. Firstly, this paper explores the evolutionary trend of motion states for surrounding vehicles in the near future, predicts the instantaneous risk and designs the ideal lane-changing trajectory to overcome the lag of static or online data. Secondly, the temporal and spatial risks are evaluated to design the virtual lane-changing trajectory curve considering the safe interaction between the SV and surrounding vehicles in a lane-changing process, which addresses the conventional risk identification defects existed in other methods. Finally, the starting and ending point determination module of lane change is designed to provide a dynamic adjustment strategy of longitudinal position before a safe lane change, which overcomes the poor flexibility of static starting and ending points in previous researches.

The rest of the paper is organized as follows. **Section 2** is the literature review. **Section 3** presents how to establish the co-evolutionary lane-changing trajectory planning model in detail. **Section 4** is the model verification part, using the lane-changing trajectory data in the real world. **Section 5** summarizes this paper and discusses the future work.

2. Literature review

Scholars have carried out a lot of work in the researches of the LTP method and obtained encouraging achievements. The prevailing methods of the LTP consist of the geometric curve, graph search, artificial potential field, etc.

2.1. Geometric curve method

The geometric curve method assumes that the vehicle follows a specific curve trajectory to complete the lane-changing process. The starting and ending state information of a lane-changing process was adopted to calibrate the parameters of the geometric curve function. The commonly used geometric curves include the polynomial curve, the circle arc curve, B-spline curves, trapezoidal curve, spiral curve, etc. Various trajectory curve models have their emphasis and the performance is quite different as well (Zhai et al., 2022).

So far, the polynomial curve is most widely used in lane-changing trajectory planning. Nelson (1989) first proposed the polynomial method for constructing vehicle trajectories. There are mainly two kinds of polynomial functions, namely polar and cartesian coordinate polynomial functions. Papadimitriou and Tomizuka (2003) established a lane-changing model under obstacles by increasing the highest power of longitudinal motion polynomial based on a polynomial algorithm. Zhang et al. (2013) adopted the time-dependent cubic polynomial equation and proposed a cost function considering the driving comfort and efficiency to optimize the lane-changing trajectory. Liu et al. (2019) employed the quintic polynomial equation to design the lane-changing trajectory of intelligent vehicles and proposed a lane-changing collision avoidance strategy based on linear tracking control. Wang et al. (2021) established a series of polynomial equations based on real-time road information and vehicle motion state and solved the unknown equation parameters by Newton iterative method to generate lane-changing trajectory dynamically. Zhang et al. (2012) used a spiral curve to describe a lane-changing trajectory, in which the change of curvature was determined by distance rather than time. Zeng et al. (2019) selected control points in advance, set vehicle collision

avoidance constraints and planned the lane-changing trajectory with continuous curvature by using a cubic B-spline curve.

2.2. Graph search method

The basic principle of the graph search method is to discretize the three-dimensional space into a graph and obtain an optimal path between two points by traversing the state space, which transforms the trajectory planning problem into a search problem in the grid graph (Zhai and Wu, 2021). The graph search method applied in vehicle trajectory planning problems is usually divided into heuristic and ergodic methods, among which Dijkstra and A* algorithm are the most common path search methods (Dijkstra, 1959; Duchon et al., 2014). BOHREN et al. (2008) modeled a discrete grid to describe the space and adopted the Dijkstra algorithm to solve the vehicle trajectory planning problem. Ziegler and Stiller (2009) used the state grid algorithm to divide the plane space into multiple grid maps and generated the lane-changing trajectory with the shortest path algorithm. McNaughton et al. (2011) transformed the structured road into a state grid space to solve the vehicle trajectory planning problem with mobile traffic flow. However, it is hard for the vehicle trajectory generated by the graph search method to guarantee the continuity of first-order or high-order, resulting in a solution dilemma in terms of the vehicle trajectory planning problem with nonholonomic constraints.

2.3. Artificial potential field method

The artificial potential field method is a common method to solve the vehicle trajectory planning problem (Khatib, 1986). This method assumes that the vehicle travels in the potential field with target points and obstacles. The target point is regarded as the center of the gravitational field to attract the subject vehicle to approach, and the obstacle is defined as the center of the repulsive field to prevent vehicle collisions. Vadakkepat et al. (2001) proposed an escape strategy to guide the solution process out of the local optimum, which aimed to improve the artificial potential field method. Li et al. (2020) proposed a vehicle lane change model based on the artificial potential field, which presented the spatial distribution of the safety potential field under different motion states during the vehicle lane-changing process. Fukuoka et al. (2013) applied the virtual electrical equation to calculate the minimum electric field between the vehicle and the obstacles, which was conducted to generate the lane-changing trajectory of anti-collision. Gan et al. (2022) adopted RS curve and potential function to deal with dynamic obstacles for autonomous vehicles during parking. In summary, the artificial potential field method has good real-time performance in planning vehicle trajectory, but it is easy to fall into local optimum in narrow traffic scenes.

2.4. Other methods

Some novel theories and methods for lane changing trajectory optimization of AVs emerge endlessly, such as game-based method, numerical solution method, etc. Fukuyama (2020) proposed a dynamic game-based method to optimize merging vehicle trajectory, and designed an algorithm to solve dynamic game based on a zero-suppressed binary decision diagram. Karimi et al. (2020) established a set of control algorithms for AV trajectory optimization in merging scenarios, while complying with the realistic constraints related to safety and comfort of vehicle occupants. Yao and Li (2021) proposed a decentralized lane change-aware AV trajectory optimization model based on a mixed traffic framework, and transformed the trajectory optimization problem into a quadratic optimization problem. Yu Bai (2021) proposed a collaborative lane change motion planning algorithm suitable for partially connected and automated environment, which is solved by a numerical solution method based on dynamic programming. Ma et al. (2021) established a bi-level optimization model based on

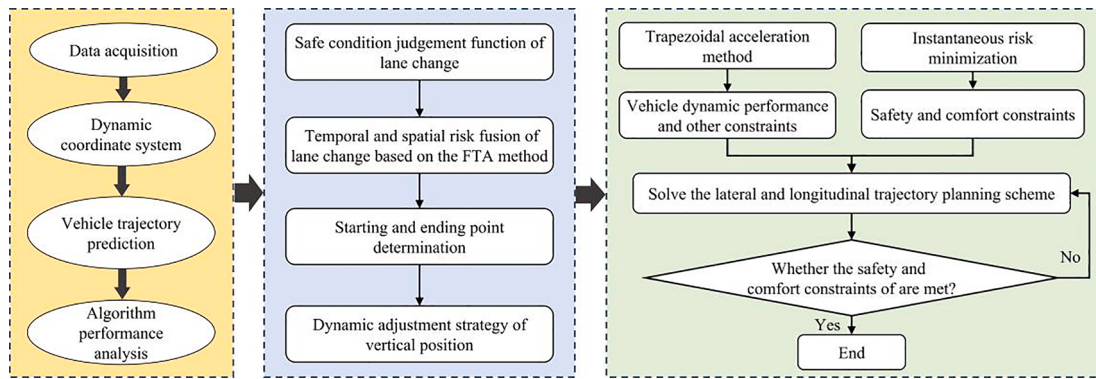


Fig. 1. The schematic diagram of the CLTP model.

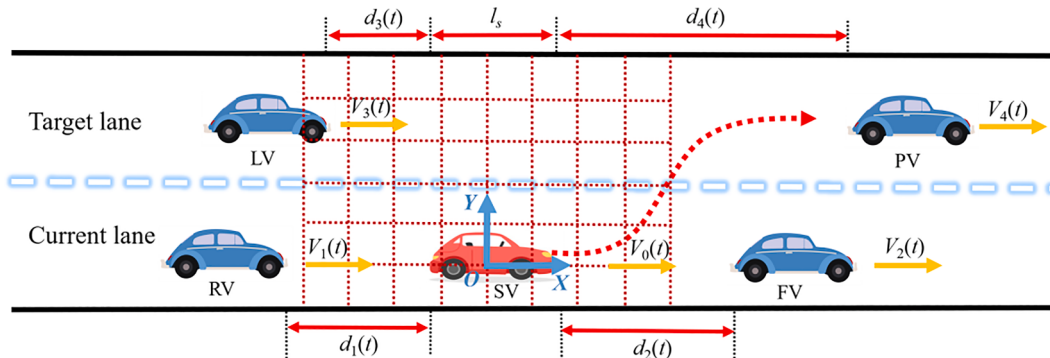


Fig. 2. A schematic illustration of a dynamic coordinate system.

discrete time to optimize the longitudinal and transverse trajectories of a single AV, and designed a parallel Monte-Carlo Tree Search algorithm to solve it. Yang et al. (2022) proposed a dynamic programming method for coordinated trajectory planning of AVs and developed a relaxation-based approximate algorithm to solve the non-convex quadratic-constrained quadratic programming problem. Mehrdad et al. (2022) established a cooperative distributed algorithm to find the optimal lane change trajectories based on predictive information from surrounding vehicles, and proposed a mixed integer programming to control the movements of AVs. The above researches have made great progress in terms of the efficiency, stability and security of AVs, providing a solid basis and inspiration for this research.

3. Methodology

3.1. Model framework

Lane-changing trajectory planning should be elaborately designed considering a variety of factors, including essential safety, basic comfort and definite efficiency. However, the lane change trajectory planning process of AV has a lot to do with whether the surrounding vehicles are AVs. Thanks to the stable and predictable motion state of AVs, the uncertainty of the lane-changing process is controllable when the adjacent vehicles of the SV are AVs. At this time, the motion state of surrounding vehicles does not have obvious randomness, so it is unnecessary to adopt deep learning method to capture the future trajectory of surrounding vehicles. Thus, the proposed model is more suitable for lane-changing scenarios where the surrounding vehicles are manual driving vehicles, that is, mixed lane change scenarios of manual driving vehicles and automatic driving vehicles. In this study, a CLTP model is proposed to address the existing limitations of current researches, as shown in Fig. 1.

The evolutionary trend of the traffic conditions around the SV is explored to judge whether the SV stays in a safe lane change status. If the

traffic condition is unsafe, the temporal and spatial risks of the SV are deduced to evaluate lane-changing safety based on the predicted vehicle trajectories. To help the SV prepare for a safe lane change, the starting and ending point positions can be obtained by using the longitudinal position adjustment strategy based on the stopping distance index (SDI). The lateral and longitudinal trajectories of lane change are designed based on the trapezoidal acceleration (TA) method and genetic algorithm (GA), which aim to reduce the overall risk coefficient of a lane-changing scheme under the constraints of given curvature, speed and instantaneous risk. However, the risk optimization process always co-evolves with the evolutionary trend of the dynamic traffic environment. Once the SV decides to accept the optimized scheme and implement the planned trajectory, it is favorable for vehicles to avoid a severe conflict or a dangerous collision, and improve the safety and reliability of the local traffic flow.

3.2. Trajectory prediction module of surrounding vehicles based on gated recurrent unit (GRU)

Assuming that the surrounding vehicles always keep a car-following status, the SV will gradually move from the current lane centerline to the target lane centerline during the lane changing process. Fig. 2 provides a structure of the dynamic coordinate system that takes the current position of SV as the origin, presenting a visual overview of the position of all vehicles and the relative distance between the SV and surrounding vehicles. The positive X-axis represents the moving direction of the SV, while the positive Y-axis indicates the left side of the SV. As the vehicle-to-vehicle communication develops, more accurate information can be acquired in an effective range via some promising equipment like radars and lasers. Therefore, the maximum detection distance should be pre-supposed and revealed by the value range of the X-axis and Y-axis. However, the dynamic coordinate system is evenly divided into $m \times n$ cells and is specified as:

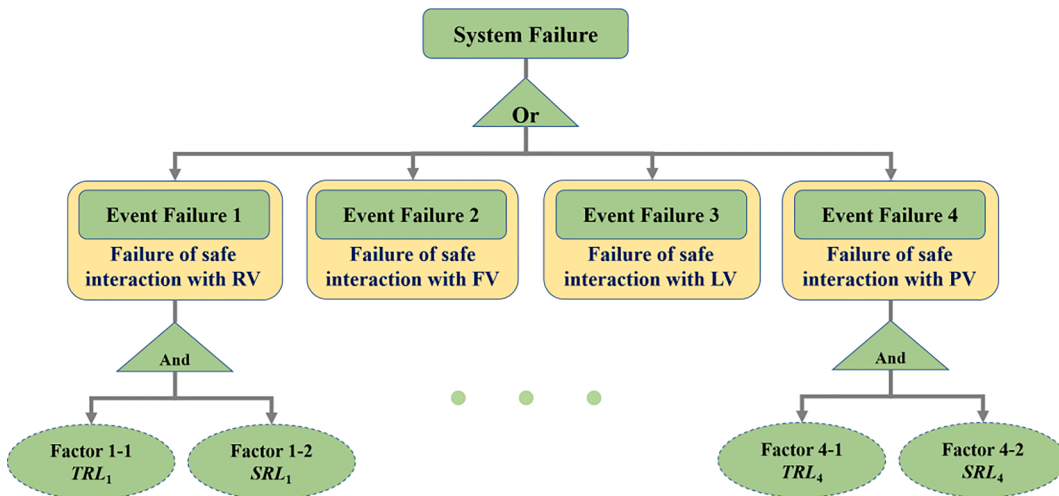


Fig. 3. The basic framework of the FTA to perform a safe interaction of the lane-changing behavior.

$$-S = x_0 < \dots < x_j < \dots < x_n = S \quad (1)$$

$$-E = y_0 < \dots < y_i < \dots < y_m = E \quad (2)$$

where x_j denotes the x-coordinate for the boundary line of column j th and y_i denotes the y-coordinate for the boundary line of row i th. S and E are the maximum longitudinal and lateral detection distances of SV respectively. m and n are both positive integers to ensure that the length and width of each cell are less than the width of any vehicles, for the sake of the arrival of vehicles. Once the vehicles occupy any part of the cell or the whole one, it can be viewed that the vehicles reach the cell.

To locate the vehicles more precisely, an approximate method is applied to simplify the location of each surrounding vehicle k . Cell (x_{ij}^k, y_{ij}^k) is adopted to indicate the cell coordinate of vehicle k is column j in row i . Thus, the centroid coordinates of Cell (x_{ij}^k, y_{ij}^k) can be obtained as follow:

$$x_{ij}^k = \frac{x_j^k + x_{j+1}^k}{2}, y_{ij}^k = \frac{y_i^k + y_{i+1}^k}{2} \quad (3)$$

To accurately obtain the motion trend of surrounding vehicles, a promising GRU algorithm is used to predict the short-term trajectory of surrounding vehicles. GRU is an improved model of recurrent neural networks (RNN). It aims to solve the problems of gradient disappearance in long-term memory and back-propagation by introducing a reset gate, update gate and input modulation gate, which can slightly modify the state flow and input flow of historical data. Therefore, compared with long short-term memory (LSTM) and RNN, GRU is easier to train and shows better training efficiency and performance.

The hidden unit in GRU is a special cell structure, which contains two gates, namely the reset gate and update gate. The reset gate is adopted to determine how to combine the new input information with the previous memory, while the update gate is mainly used to control how many previous memories are stored to the current time step. Let x_t^k denote the coordinate of surrounding vehicle k at time t , that is, $x_t^k = (x_{ij}^k, y_{ij}^k)$. GRU is employed to predict the motion trajectory of surrounding vehicles, and the calculating process of each door control is as follows:

$$r = \sigma(x_{t+1}^k U^r + s_t^k W^r) \quad (4)$$

$$z = \sigma(x_{t+1}^k U^z + s_t^k W^z) \quad (5)$$

$$h = \tanh(x_{t+1}^k U^h + (s_t^k \otimes r) W^h) \quad (6)$$

$$s_{t+1}^k = z \otimes s_t^k + (1 - z) \otimes h \quad (7)$$

where r is the reset gate, z is the update gate and h is the current memory content. s_t^k is the final memory of surrounding vehicle k at the current time step, σ is sigmoid activation function, x_t^k is the observed data of surrounding vehicle k at time t , U^i refers to the update transfer matrix and W^i denotes the weight matrix, $i = r, z, h$. The symbol \otimes indicates that the elements in the corresponding positions of two vectors are multiplied.

3.3. Instantaneous risk identification module of AV in a lane change

3.3.1. Safety status determination function based on SDI index in a lane change

As a preliminary step, it is essential to know whether the AV encounters risky status in a given lane-changing condition, which has a significant impact on traffic accident prevention. Due to high traffic density, it's common that the SV intending to change to a higher speed lane is surrounded by several vehicles. When changing lane, drivers are supposed to concentrate more on the traffic environment and the dynamic interaction with the surrounding vehicles to keep a safe distance headway and vehicle motion state. Otherwise, dangerous accidents or conflicts are more likely to happen. Previous study has proved that vehicle space series features can be effectively used to estimate the crash risk level of a lane change event in advance (Chen et al., 2020). Thus, this study introduces a popular and practical distance index SDI to resolve this problem. Once the future trajectories of surrounding vehicles are provided by GRU, it can judge whether the SV may collide at the predicted time $t|t+k$ in a lane change. A safety status determination function is given as follows:

$$P[s_{t|t+k}^0, s_{t|t+k}^i] = \begin{cases} \text{safe For anyi, it satisfies } SDI_i(t|t+k) \geq 0 & i = 1, 2, \dots, n \\ \text{unsafe otherwise} \end{cases} \quad (8)$$

where $s_{t|t+k}^0$ and $s_{t|t+k}^i$ represent the positions of SV and surrounding vehicle i at the predicted time $t|t+k$, respectively. $SDI_i(t|t+k)$ indicates the stopping distance index between the SV and surrounding vehicle i at the predicted time $t|t+k$.

In the process of evaluating lane-changing risk, every SDIs between the SV and surrounding vehicles should be calculated at first. However, there may exist various position relationships among vehicles. For instance, the SV is in the rear position compared with the FV and PV, while in the forward position compared with the RV and LV. To put it simply in the calculation, two special labels, forward and back position are used to explain the complex relative position relationship. After that, all SDIs can be easily obtained as:

$$SDI_i(t|t+k) = D_F(t|t+k) - D_R(t|t+k) + d_i(t|t+k) - l_F \quad (9)$$

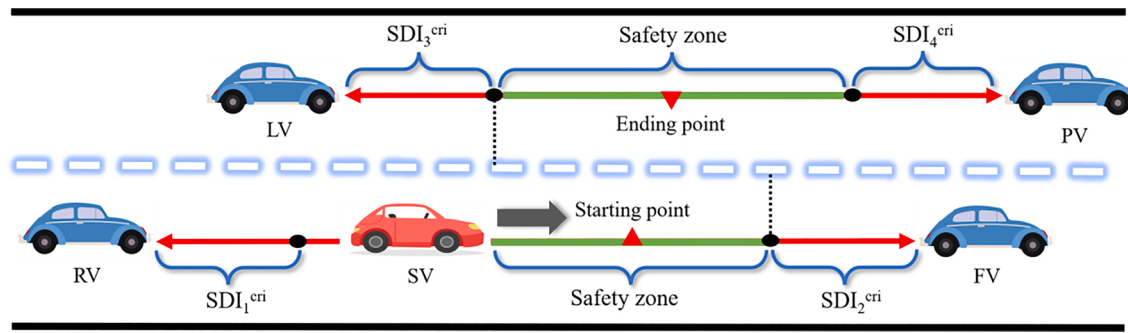


Fig. 4. Starting and ending point determination strategy based on critical safety distance constraint.

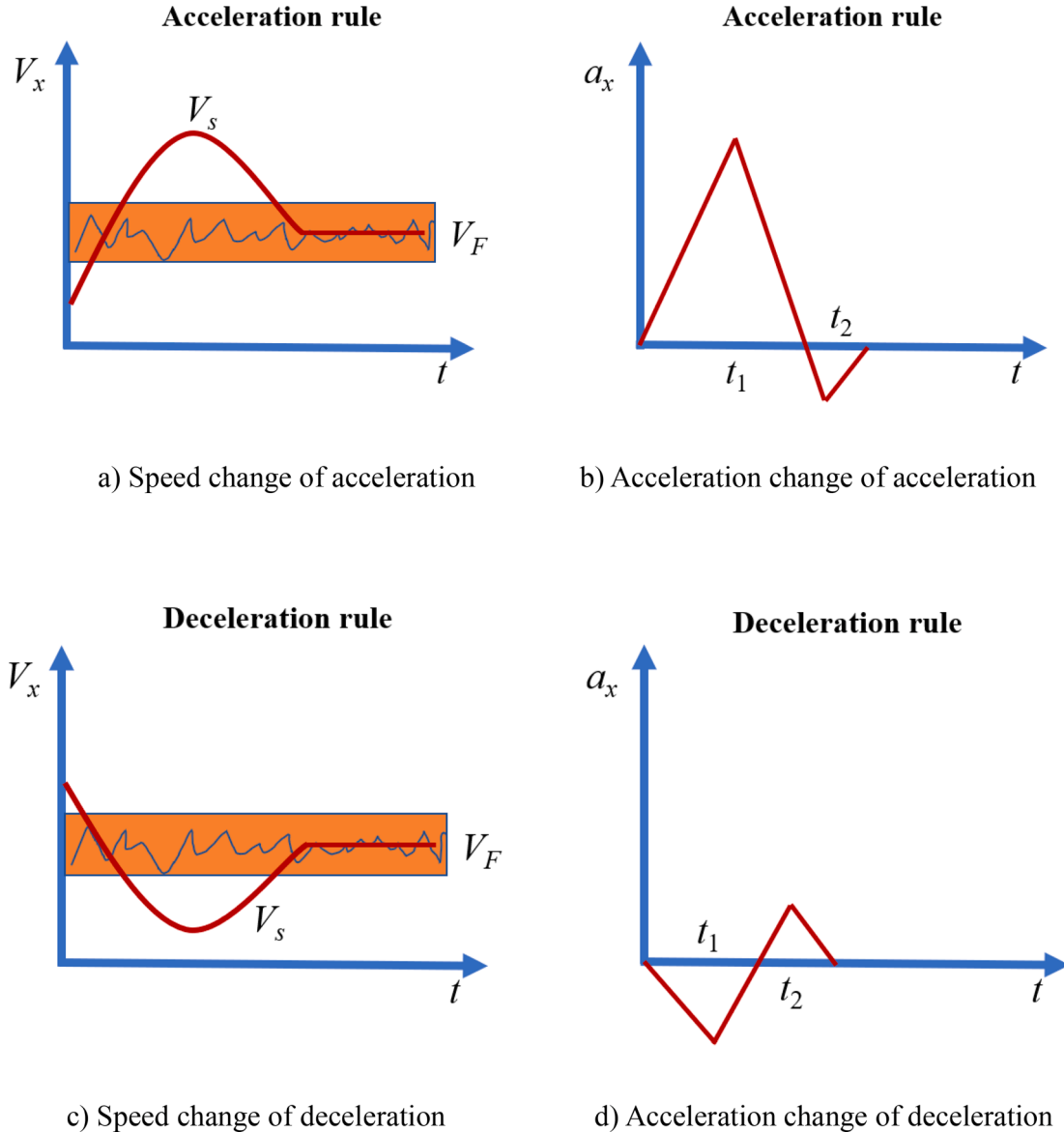


Fig. 5. Speed and acceleration changes of the SV under different driving behaviors.

$$D_j(t|t+k) = \frac{V_j^2(t|t+k)}{254 \times (f \pm g)} + t_r \times V_j(t|t+k) \times 0.278, j = 0, 1, \dots, n \quad (10)$$

where $D_F(t|t+k)$ is the stopping sight distance (SSD) of the vehicle in the forward position between the SV and surrounding vehicle i at the predicted time $t|t+k$. $D_R(t|t+k)$ is the SSD of the vehicle in the rear position between the SV and surrounding vehicle i at the predicted time $t|t+k$. $D_j(t|t+k)$ denotes the SSD of the vehicle j (including the SV and surrounding vehicles, $j = 0$ represents the SV) at the predicted time $t|t+k$. $d_i(t)$ denotes the longitudinal distance between the SV and surrounding vehicle i at the predicted time $t|t+k$. l_F denotes the length of

predicted time $t|t+k$. $D_R(t|t+k)$ is the SSD of the vehicle in the rear position between the SV and surrounding vehicle i at the predicted time $t|t+k$. $D_j(t|t+k)$ denotes the SSD of the vehicle j (including the SV and surrounding vehicles, $j = 0$ represents the SV) at the predicted time $t|t+k$. $d_i(t)$ denotes the longitudinal distance between the SV and surrounding vehicle i at the predicted time $t|t+k$. l_F denotes the length of

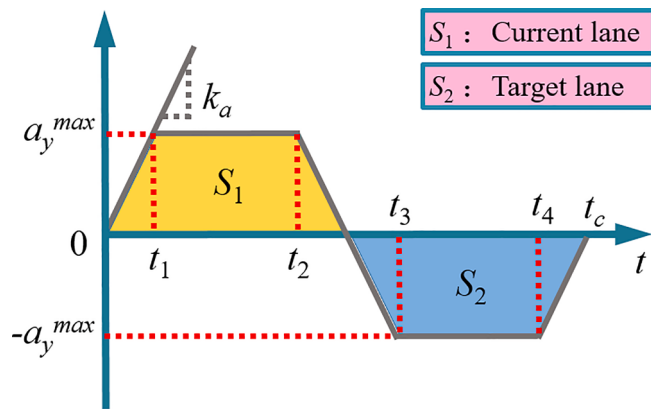


Fig. 6. The trapezoidal acceleration curve.

the vehicle in the forward position, which is generally regarded as a standard vehicle and valued at 3.5 m. f denotes surface friction coefficient, which is regularly valued as 0.6 on the highway. t_r denotes the driver perception time, which is generally selected as 2.5 s (Wang et al., 2018). g denotes road grade.

3.3.2. Temporal and spatial risk fusion of AV based on the fault tree analysis (FTA) method

If there is a potential collision risk in current traffic conditions, it is necessary to make a detailed assessment of the temporal and spatial risks of the SV. A risk identification method based on the FTA method is proposed to comprehensively quantify the temporal and spatial risks, as shown in Fig. 3.

As an important method of risk analysis in safety system engineering, the FTA is a logical deductive system evaluation method that can be both

qualitative and quantitative. It is usually used to explore the relationship between the failure of the whole system and the failure of each event (Gardoni, 2017). For the lane-changing behavior, system failure is defined as the failure of a safe interaction between the SV and all surrounding vehicles. When the SV moves to different positions, there are significant differences in the lane-changing interaction between them. Thus, according to the relative position relationship between the SV and lane line, there are two calculation forms of the instantaneous risk coefficient that can be further discussed. Before the SV crosses the lane line, the instantaneous risk coefficient is affected by four surrounding vehicles i ($i = 1, \dots, n, n \leq 4$) at most that may continuously interact with the SV. In this case, the instantaneous risk coefficient will be derived from four values of the possible failure events of safe interaction at most. Once the SV completely crosses the lane line, the instantaneous risk coefficient is only affected by the PV and LV in the target lane. The reason is that the SV only interacts with the PV and LV in the target lane

Table 1
Comparison of prediction errors for different models.

Vehicles	Model	Training set			Test set		
		RSME	MAE	MAPE	RSME	MAE	MAPE
FV	GRU	2.392	1.671	0.67 %	2.262	1.717	0.67 %
	ANN	2.630	1.698	0.68 %	2.411	1.563	0.61 %
	LSTM	2.457	1.723	0.69 %	2.323	1.772	0.69 %
	GRU	2.446	1.942	0.76 %	2.325	1.917	0.76 %
RV	ANN	3.045	2.196	0.88 %	3.248	2.216	0.89 %
	LSTM	2.541	1.985	0.78 %	2.304	1.900	0.75 %
	GRU	2.306	1.745	0.67 %	2.226	1.696	0.65 %
PV	ANN	2.803	1.950	0.77 %	2.515	1.738	0.67 %
	LSTM	2.551	1.924	0.73 %	2.405	1.825	0.69 %
	GRU	1.938	1.459	0.58 %	1.801	1.475	0.59 %
LV	ANN	2.324	1.429	0.57 %	2.230	1.352	0.54 %
	LSTM	2.026	1.536	0.61 %	1.870	1.544	0.62 %

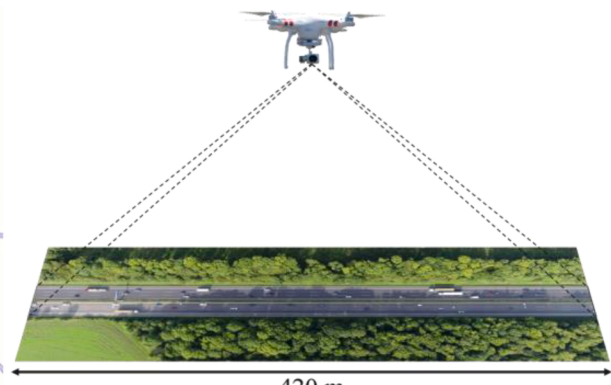


Fig. 7. Collection location and range of Cologne highway in Germany.

A lane change sample

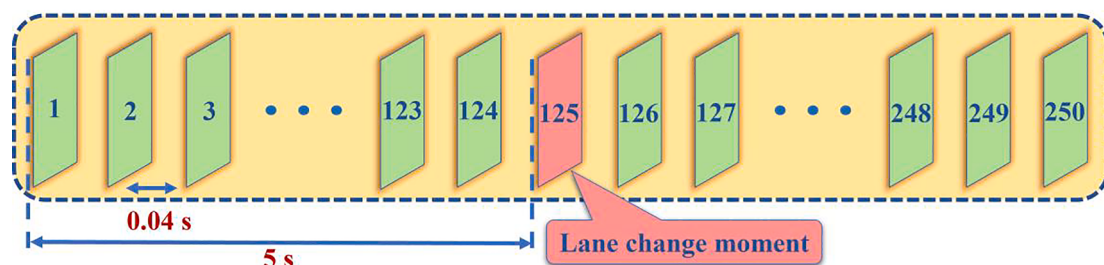


Fig. 8. The schematic diagram of the composition for a lane change sample.

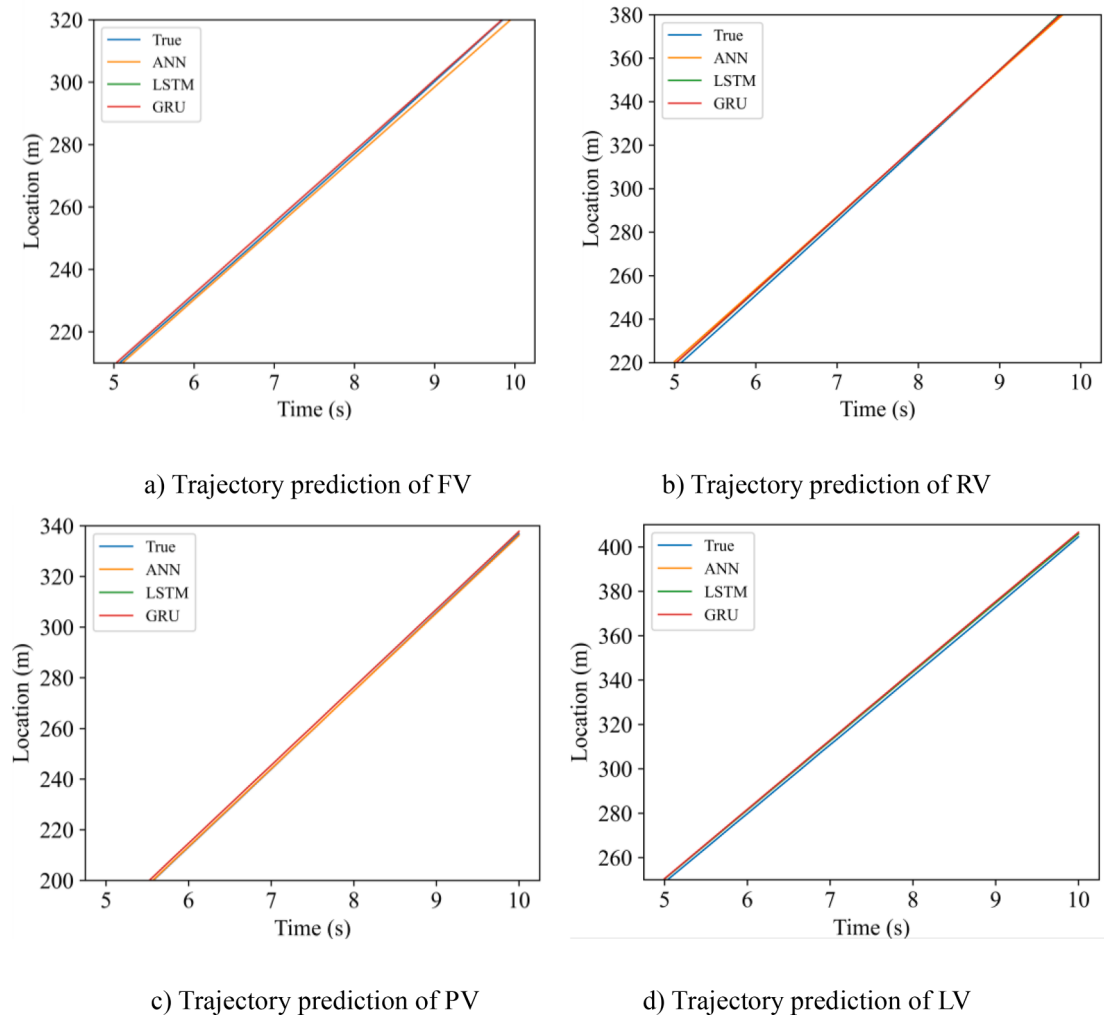


Fig. 9. Prediction results of surrounding vehicle trajectory.

and has nothing to do with the surrounding vehicles ($i = 1, 2$) in the original lane. In this case, the instantaneous risk coefficient will be derived from two values of the possible failure events of safe interaction at most.

According to our previous research (Wu et al., 2020), the FTA is an effective method to integrate the temporal and spatial risks in a lane-changing process, and the associated recognition accuracy rate of the risky lane changes and traffic conflicts can be more than 97 %. Therefore, this study adopts FTA to quantify the instantaneous risk of lane change, and the instantaneous risk coefficient $\varphi_s(t|t+k)$ of SV at the predicted time $t|t+k$ can be obtained as follows:

$$\varphi_s(t|t+k) = \begin{cases} 1 - \prod_{i=1}^4 [1 - \eta_i(t|t+k)], & \text{before SV crosses the lane line} \\ 1 - [1 - \eta_3(t|t+k)] \times [1 - \eta_4(t|t+k)], & \text{After SV crosses the lane line} \end{cases} \quad (11)$$

$$\eta_i(t|t+k) = TRL_i(t|t+k) \times SRL_i(t|t+k) \quad (12)$$

where $\eta_i(t|t+k)$ denotes the event's failure possibility of safe interaction between the SV and surrounding vehicle i ($i = 1, \dots, n$, $n \leq 4$) at the predicted time $t|t+k$. $TRL_i(t|t+k)$ denotes the temporal risk level between the SV and surrounding vehicle i ($i = 1, \dots, n$) at the predicted time $t|t+k$, and tends to reflect collision probability. $SRL_i(t|t+k)$ denotes the spatial risk level between SV and surrounding vehicle i ($i = 1, \dots, n$) at the predicted time $t|t+k$, and usually emphasizes the severity of

a collision. The relevant calculation steps are as follows:

$$TRL_i(t|t+k) = e^{-\frac{TTC_i^2}{2\sigma^2}} \quad (13)$$

$$TTC_i = \begin{cases} \frac{d_i(t|t+k)}{V_i - V_s}, & \text{if } V_i > V_s \text{ and vehicle is stays behind} \\ \frac{d_i(t|t+k)}{V_s - V_i}, & \text{if } V_s > V_i \text{ and vehicle is stays ahead} \end{cases} \quad (14)$$

$$SRL_i(t|t+k) = \begin{cases} \frac{|SDI_i(t|t+k)|}{SDI_i^{cri}(t|t+k)} SDI_i(t|t+k) 0 \\ 0 SDI_i(t|t+k) \geq 0 \end{cases} \quad (15)$$

$$SDI_i^{cri}(t|t+k) = D_R(t|t+k) + l_F \quad (16)$$

where TTC_i denotes Time-To-Collision (TTC) between the SV and surrounding vehicles i ($i = 1, \dots, n$). $SDI_i^{cri}(t|t+k)$ denotes the theoretical maximum SDI at the predicted time $t|t+k$. σ is a standardization constant, which denotes the sum of average action time of drivers and effective time of the vehicle braking system. To make the model practical, σ is set as 1.5 according to the empirical value provided by the previous research (Sun and Fang, 2017).

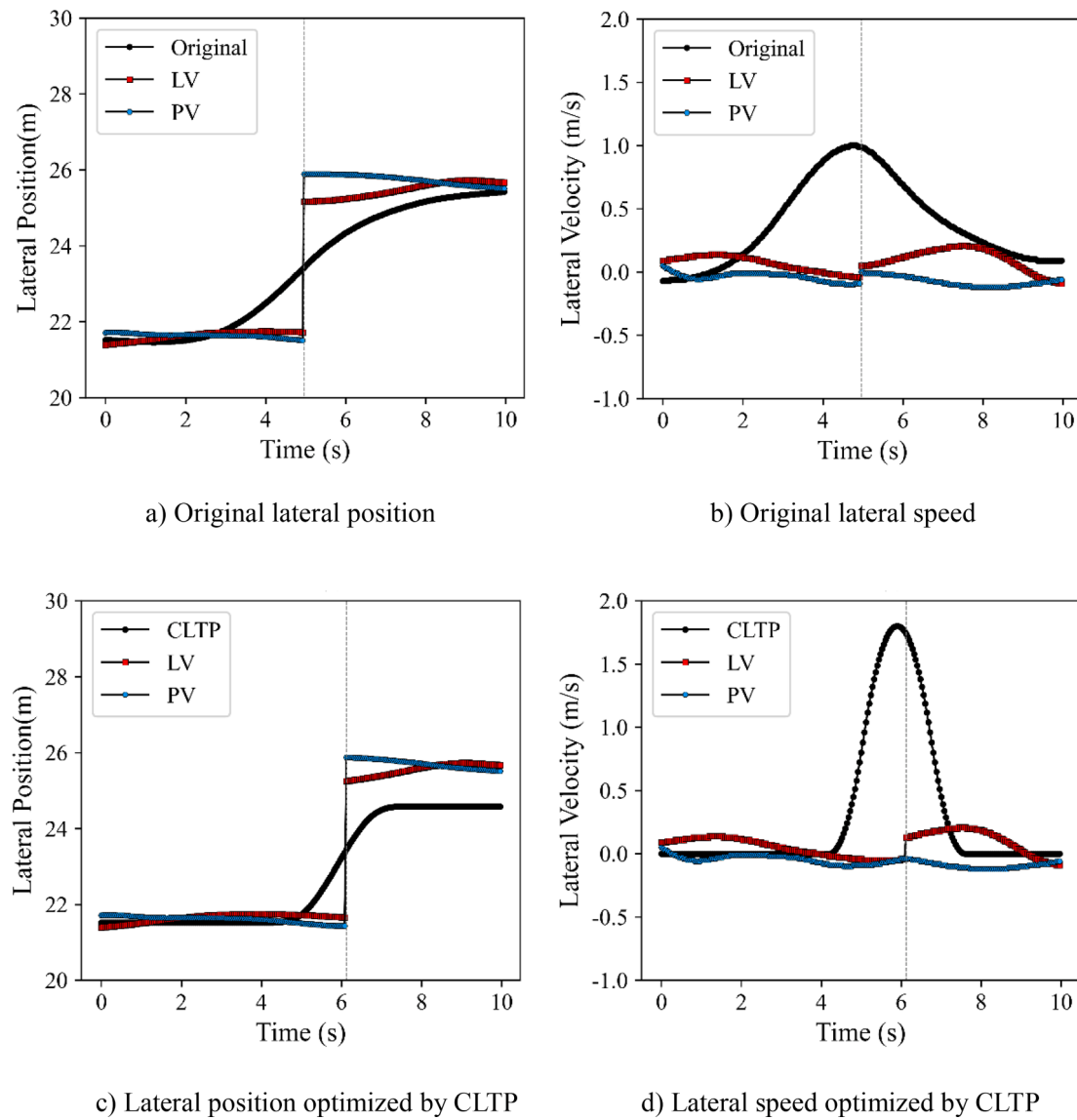


Fig. 10. Examples of lateral motion of vehicles output by original scenario and CLTP.

3.4. Trajectory generation module of AV in a lane-changing process

3.4.1. Starting and ending point determination

The choices of starting and ending points of lane-changing trajectory are closely related to the possibility of traffic conflicts for AVs. To reduce collision risk, the longitudinal position of the starting and ending points of a lane-changing trajectory should be within the safe range to avoid rollover and collision, as shown in Fig. 4.

The longitudinal position of the starting point of a lane-changing trajectory shall be selected particularly to ensure longer distance for the SV than the critical stopping sight distances from the surrounding vehicles. The calculation is as follows:

$$x_s^{start}(t_s) \geq \max \{x_1(t_s) + SDI_1^{cri}(t_s), x_3(t_s) + SDI_3^{cri}(t_s)\} \quad (17)$$

$$x_s^{start}(t_s) \leq \min \{x_2(t_s + t_c) - SDI_2^{cri}(t_s + t_c), x_4(t_s + t_c) - SDI_4^{cri}(t_s + t_c)\} \quad (18)$$

where t_s and t_c denote the beginning time of lane change for the SV and the lane change duration respectively. $x_s^{start}(t_s)$ refers to the longitudinal position when the SV starts to change lanes, $x_s^{end}(t_s + t_c)$ is the longitudinal position of the SV at the end of lane change, and x_i is the

longitudinal position of the surrounding vehicle i , $i = 1, 2, 3, 4$.

The longitudinal position of the ending point for the SV is usually related to the motion state of the PV and LV, which is supposed to be within the intersection range between the critical SSDs of the PV and LV in the target lane, as shown in Eq. (18).

$$x_3(t_s + t_c) + SDI_3^{cri}(t_s + t_c) \leq x_s^{end}(t_s + t_c) \leq x_4(t_s + t_c) - SDI_4^{cri}(t_s + t_c) \quad (19)$$

To select reasonable starting and ending positions of a safe lane change, the speed control scheme in the optimal trajectory solution algorithm can be adjusted by setting reasonable acceleration and deceleration rules for AVs. As shown in Fig. 5, when the ideal starting point of lane change is in front of or behind the SV, the SV tends to reach the associated positions according to specific acceleration or deceleration rules, eventually keeping a similar speed with the vehicle in front.

3.4.2. Lateral trajectory planning based on the TA method

To relax the untrue assumptions of speed and acceleration in the model, the trapezoidal acceleration curve is adopted to design a smooth lateral trajectory of the SV. Fig. 6 shows the trapezoidal acceleration curve of the lateral movement of the SV (Jie et al., 2018). It can be seen that if the maximum values and the change rate of lateral acceleration of the SV are given, the lateral acceleration a_y in a lane-changing event can

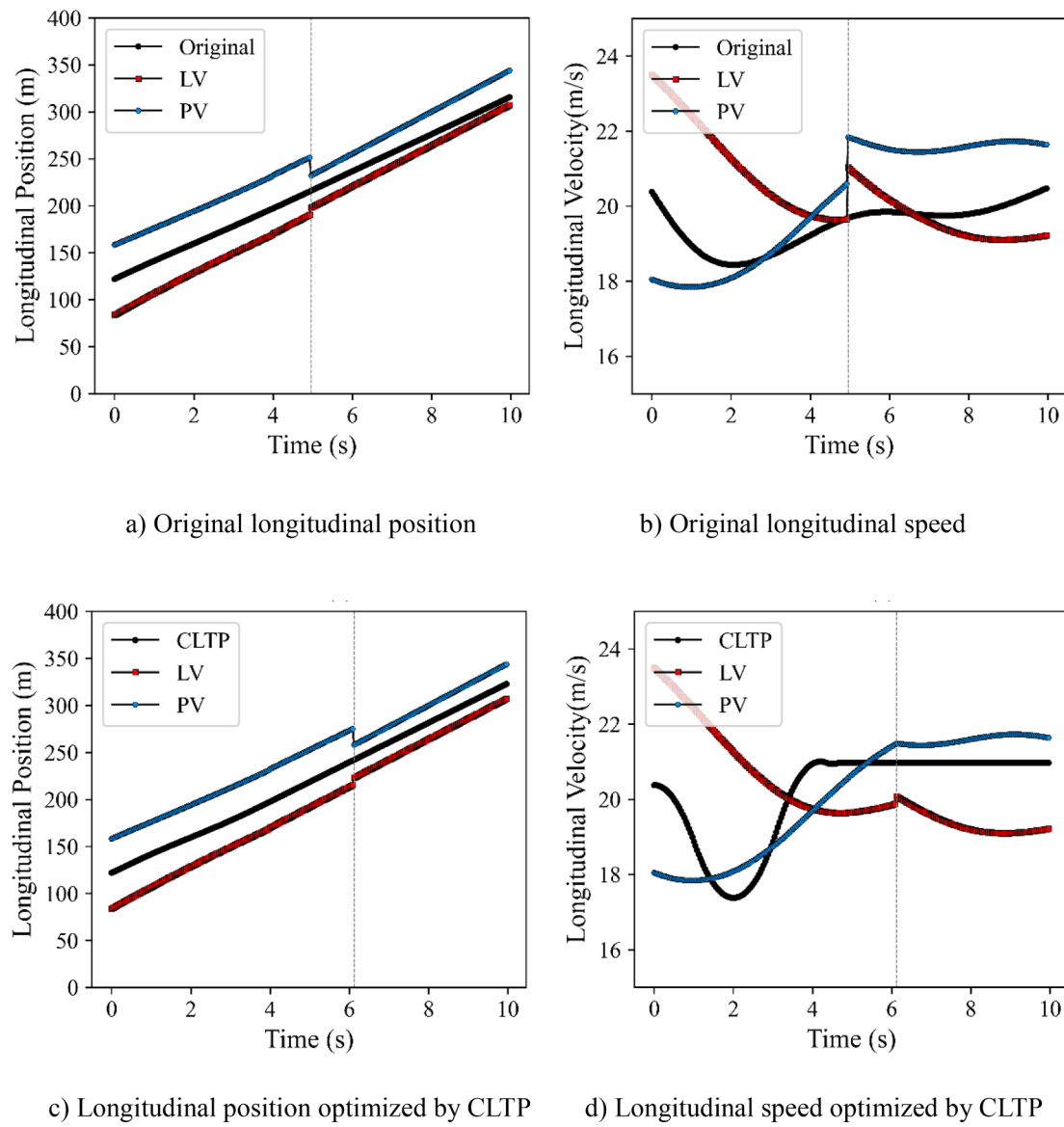


Fig. 11. Examples of longitudinal motion of vehicles output by original scenario and CLTP.

Table 2
Statistical results of φ_s output by different methods.

	Maximum	Minimum	Mean	Median	Standard
Original	0.5881	0	0.0004	0	0.0105
SLTP	0.9929	0	0.006	0	0.0519
CLTP	0.2817	0	2.41×10^{-5}	0	0.0021

be organized as follows:

$$a_y^{max} = k_a f(t) - k_a(t-t_1)f(t-t_1) - k_a(t-t_2)f(t-t_2) + k_a(t-t_3)f(t-t_3) + k_a(t-t_4)f(t-t_4) - k_a(t-t_c)f(t-t_c) \quad (20)$$

where a_y^{max} is the maximum lateral acceleration of the SV, k_a is the change rate of lateral acceleration of the SV, t is the time variable at the future moment, $f(t)$ is the unit step function. t_1 , t_2 , t_3 and t_4 are transient time variables, t_1 and t_2 are the starting and ending instants when the SV reaches the maximum lateral acceleration, t_3 and t_4 are the starting and ending instants when the SV reaches the minimum lateral acceleration.

Assume the lateral displacement of the SV on the original lane is

equal to that on the target lane. D denotes the horizontal spacing between the center lines of the two lanes. The relationships are as follows:

$$t_1 = \frac{t_3 - t_2}{2} = t_c - t_4 = \frac{a_y^{max}}{k_a} \quad (21)$$

$$t_2 - t_1 = t_4 - t_3 \quad (22)$$

$$t_2 = -\frac{a_y^{max}}{2k_a} + \sqrt{\left(\frac{a_y^{max}}{2k_a}\right)^2 + \frac{D}{k_a}} \quad (23)$$

The quadratic integration of Equation (23) is carried out and then Equations (21) and (22) are substituted into the integration formula. The following relationship can be obtained:

$$D = \frac{t_c^2 a_y^{max}}{4} - \frac{t_c \left(a_y^{max} \right)^2}{2k_a} \quad (24)$$

The lateral trajectory design of lane change is also subject to the following constraints:

- (1) To meet the requirements of comfort and vehicle motion performance constraints, the maximum lateral acceleration of the vehicle is:

$$-a_y^{\max} \leq a_y \leq a_y^{\max} \quad (25)$$

According to the design parameters of vehicle motion performance, it is assumed that the maximum lateral acceleration and its change rate of the vehicle are $a_y^{\max} = 3 \text{ m}\cdot\text{s}^{-2}$ and $k_a = 5 \text{ m}\cdot\text{s}^{-3}$.

(2) Since there is a driving risk if the lane-changing duration is too long or too short, it is necessary to restrict the related value range:

$$t_{\min} < t_c \leq t_{\max} \quad (26)$$

[Yao et al. \(2016\)](#) give a typical lane change duration of 6 s that follows a normal distribution and selects 3–10 s as the lane change time range, which is $t_{\min} = 3 \text{ s}$ and $t_{\max} = 10 \text{ s}$.

(3) The centerline interval between the original lane and the target lane is the external environmental constraint of lane-changing trajectory planning. In this paper, the standard lane width $D = 3.75 \text{ m}$ is selected as the model reference value.

3.4.3. Longitudinal trajectory planning based on risk minimization

The CLTP model aims to minimize the total risk coefficient of the lane-changing trajectory of the SV, and ensure the stability of local traffic flow. Moreover, the longitudinal speed of the SV will be dynamically adjusted with the future trajectory change of surrounding vehicles under the premise of minimizing the instantaneous risk and meeting the requirements of comfort and speed. Therefore, the optimization objective of longitudinal trajectory is:

$$\begin{aligned} \min \int_t^{t+t_c} g(t+\tau) d\tau &= \int_0^{t_c} \varphi_s(t+\tau) + M_1(TRL_i(t+\tau) - \delta_1) + M_2(SRL_i(t+\tau) - \delta_2) d\tau \\ &= \int_t^{t+t_c} M_1(TRL_i(t+\tau) - \delta_1) + M_2(SRL_i(t+\tau) - \delta_2) + 1 - \prod_{i=1}^n [1 - \eta_i(t+\tau)] d\tau \end{aligned} \quad (27)$$

where $g(t+\tau)$ is the lane-changing risk of the SV at the predicted time $t+\tau$; n is the number of surrounding vehicles ($n \leq 4$); M_1 and M_2 are the penalty coefficients of temporal and spatial risks between SV and surrounding vehicles at the predicted time $t+\tau$ respectively, and their values are temporarily set to 3; τ is any moment within the lane change duration t_c ; δ_1 and δ_2 are the safe thresholds of temporal and spatial risks.

To meet the requirements of the safety distance, speed limit and

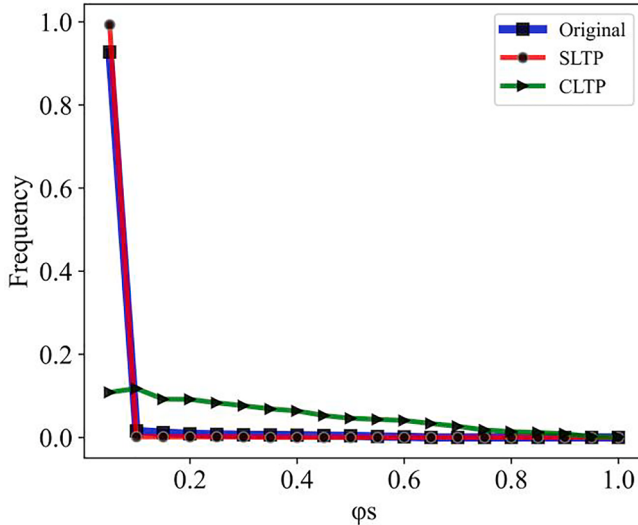


Fig. 12. Scatter diagram of instantaneous risk coefficient φ_s for all lane-changing samples.

Table 3

Statistical results of TTCs between SV and surrounding vehicles in the lane change events.

		Maximum	Minimum	Average	Median	Standard
FV	Original	6705	0.03	39.19	14.36	164.75
	SLTP	103,030	3.39	74.03	19.38	940.11
	CLTP	231,240	2.97	204.97	24.37	2860.75
RV	Original	12,732	4.11	135.14	39.53	401.36
	SLTP	246,930	0.02	133.97	17.89	2656.19
	CLTP	123,530	5.09	169.57	33.39	1965.21
PV	Original	10,743	2.47	95.12	31.74	312.70
	SLTP	63,223	0.25	199.01	56.62	1306.09
	CLTP	131,510	6.54	413.73	54.43	3462.30
LV	Original	12,743	0.04	73.59	22.82	278.05
	SLTP	92,642	0.01	49.71	6.05	995.61
	CLTP	150,410	2.38	229.87	26.88	3033.44

comfort, the longitudinal trajectory should meet the following constraints:

$$0 < V_S(t+\tau) \leq V_L \quad (28)$$

$$|a_x(t+\tau)| \leq a_L \quad (29)$$

where $V_S(t+\tau)$ is the longitudinal speed of SV at the predicted time $t+\tau$; V_L is the maximum longitudinal speed limit of SV; $a_x(t+\tau)$ is the longitudinal acceleration of the SV at the predicted time $t+\tau$ and a_L refers

to the maximum longitudinal acceleration of the SV under the premise of driving comfort.

4. Results and discussion

4.1. Data source and processing

To verify the effectiveness of the CLTP model, the vehicle trajectory data provided by HighD project is adopted to conduct the comparative analysis ([Krajewski et al., 2018](#)). The dataset records traffic conditions of six different sections of Cologne Expressway in Germany with the unmanned aerial vehicle, and extracts the vehicle motion trajectory data using computer vision and machine learning algorithm. As shown in [Fig. 7](#), the length of the road section is 420 m. The recognition error of vehicle position is 10 cm, and the sampling period is 25 frames per second. The dataset contains 110,500 vehicles with cumulative driving distance of 44,500 km and driving time of 147 h. Each frame involves 26 attributes, including vehicle number, frame number, horizontal and vertical coordinates, vehicle type, vehicle size, speed, acceleration, surrounding vehicle number, lane number, etc.

Since the lane change behavior is a continuous process, a lane-changing sample that involves 5 vehicles at most should consist of a

Table 4

Statistical results of TIT between the SV and surrounding vehicles in lane change events.

	Maximum	Minimum	Average	Median	Standard
Original	5.4730	0.0000	1.3528	0.9901	1.2029
SLTP	5.4939	0.0006	2.8581	2.9266	1.5687
CLTP	5.2191	0.0008	1.0754	0.3634	1.3577

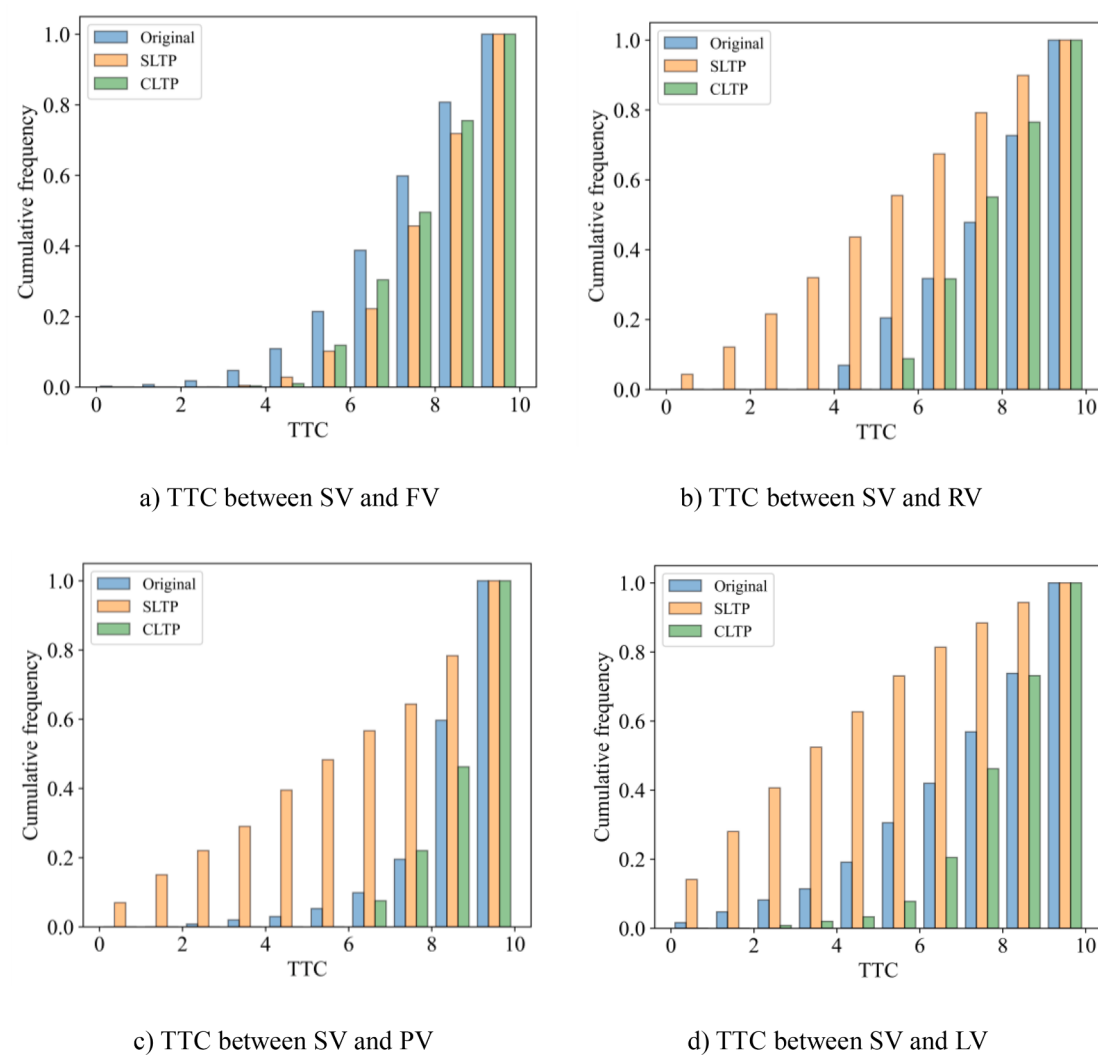


Fig. 13. The cumulative frequency diagrams of TTCs between the SV and surrounding vehicles.

Table 5

Statistical results of SDI between the SV and surrounding vehicles in the lane change events.

		Maximum	Minimum	Average	Median	Standard
FV	Original	191.19	-18.10	30.52	25.05	22.90
	SLTP	190.43	0.73	35.98	30.35	23.65
	CLTP	189.74	-2.77	37.11	32.12	23.68
RV	Original	129.06	-0.46	35.75	30.27	21.76
	SLTP	153.52	-19.83	36.64	31.66	23.41
	CLTP	147.01	-2.27	38.42	32.84	21.91
PV	Original	131.68	-14.57	33.35	28.82	23.11
	SLTP	194.92	-14.57	61.92	59.82	33.51
	CLTP	182.84	-14.57	53.35	49.23	31.97
LV	Original	211.95	-21.54	41.22	36.02	27.63
	SLTP	251.28	-73.89	37.47	33.38	39.57
	CLTP	254.28	-13.92	54.94	49.82	35.23

series of consecutive frames of data. According to the data formats, the lane-changing moment is defined as the time when the vehicle centroid crosses the lane line. To unify the sample format and avoid losing important information, the sample length of a lane change must be large enough and exceeds the duration of most lane change events. In this paper, the 5 s before and after the lane-changing moment (250 frames in total) are regarded as the starting and ending time of a lane change sample, as shown in Fig. 8. The cycle time of lane change sample data is

Table 6

Statistical results of MTC between the SV and surrounding vehicles in the lane change events.

		Maximum	Minimum	Average	Median	Standard
FV	Original	46.52	0.17	4.84	3.29	4.10
	SLTP	108.65	0.17	6.93	5.55	5.27
	CLTP	44.18	0.17	5.58	4.24	3.86
RV	Original	12.32	0.37	3.06	2.56	1.67
	SLTP	13.03	0.04	3.05	2.59	1.71
	CLTP	13.64	0.41	3.14	2.68	1.65
PV	Original	56.73	0.21	9.99	10.02	7.02
	SLTP	102.38	0.21	11.33	10.86	6.72
	CLTP	39.42	0.21	10.89	10.85	6.36
LV	Original	16.49	0.17	3.47	3.04	1.94
	SLTP	20.99	0.03	3.44	2.95	2.45
	CLTP	18.89	0.35	4.31	3.90	2.43

10 s, which is not equal to the duration of a lane change. To sum up, 1000 groups of samples were obtained after excluding abnormal or missing data.

4.2. Performance analysis of vehicle trajectory prediction

Root mean square error (RMSE), mean absolute error (MAE) and mean absolute percent error (MAPE) are selected as the measurement

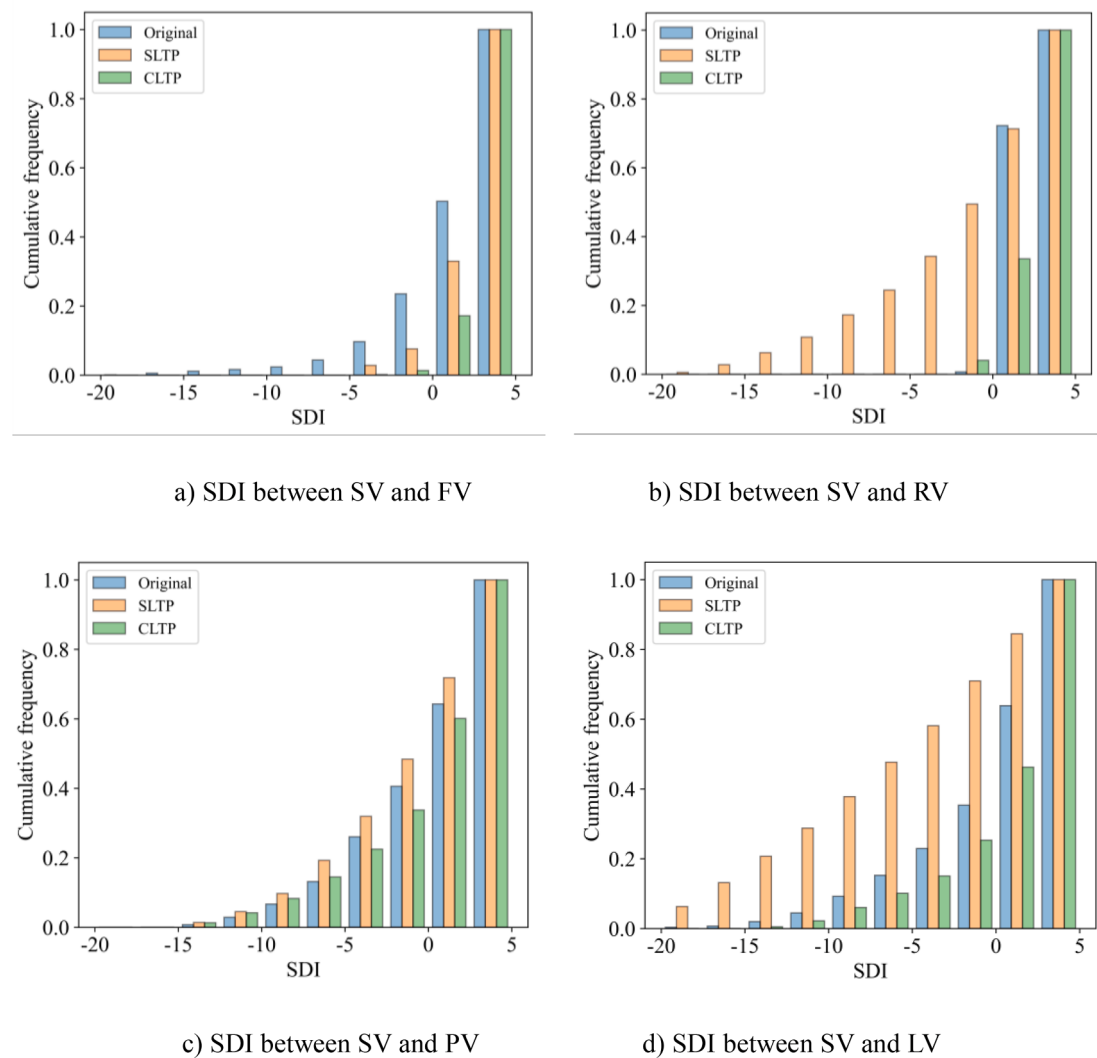


Fig. 14. Distribution of SDI between the SV and surrounding vehicles in all lane change samples.

standards for the prediction results of vehicle trajectories. The error results of GRU, ANN and LSTM models with a time window of 5 s are shown in Table 1 and Fig. 9. 70 % of the samples are used as training sets and the rest as test sets.

From Table 1 and Fig. 9, three models show good performance in predicting the trajectories of surrounding vehicles and are less than 0.9 % in terms of MAPE. Among them, the trajectory prediction method based on the GRU model has attained better performance on RSME and MAE, which is slightly better than the other two methods. It can be observed that the GRU model can ensure higher accuracy when predicting the trajectories of surrounding vehicles, and has advantages in processing long time series.

4.3. Performance analysis of vehicle motion

Examples of vehicle lateral and longitudinal motion conditions of lane change events optimized by the CLTP model are shown in Fig. 10 and Fig. 11. From the change of vehicle lateral position in Fig. 10 a) and c), the lateral displacements of the SV before and after optimization are not equal. This is because the vehicle centroid does not always coincide with the lane centerline at the beginning or ending position of a lane change in reality, while the lateral offset planned by the CLTP model is equal to the lane width. The lateral velocity in Fig. 10 c) and d) show that the lane-changing vehicle adjusts its lateral velocity dynamically. However, the lateral velocity of the SV optimized by the CLTP model is

more symmetrical and rapid, enabling the vehicle to change lanes smoothly and effectively.

As shown in Fig. 11 a) and c), the discontinuous change of vehicle longitudinal position indicates that the front and rear vehicles change as the SV overtakes. In the actual lane change, the SV is more concerned about keeping a safe distance from front vehicles, and tends to ignore the dynamic control of the distance from rear vehicles. Therefore, the CLTP model comprehensively considers the safe interaction between SV and surrounding vehicles in the lane-changing process to select the ideal starting and ending points. From Fig. 11 c) and d), the vehicle dynamically adjusts its longitudinal speed according to the rules established in the CLTP model, and gradually drives to the desired starting and ending points of a lane change, ensuring a safer and smoother lane change.

4.4. Comparative analysis of temporal and spatial risks

To verify the optimization effect of the proposed model, the instantaneous risk coefficient φ_s of the original, SLTP and CLTP methods are given to evaluate the safety of the lane-changing trajectory. The statistical results are shown in Table 2 and Fig. 12. Table 2 shows that the CLTP model significantly improves the safe interaction between the SV and surrounding vehicles, and the maximum risk coefficient of that is reduced by 52.1 % and 71.63 % respectively, compared with the Original and SLTP methods. Fig. 12 demonstrates the effective performance of the CLTP model in restraining the growth of lane-changing risk.

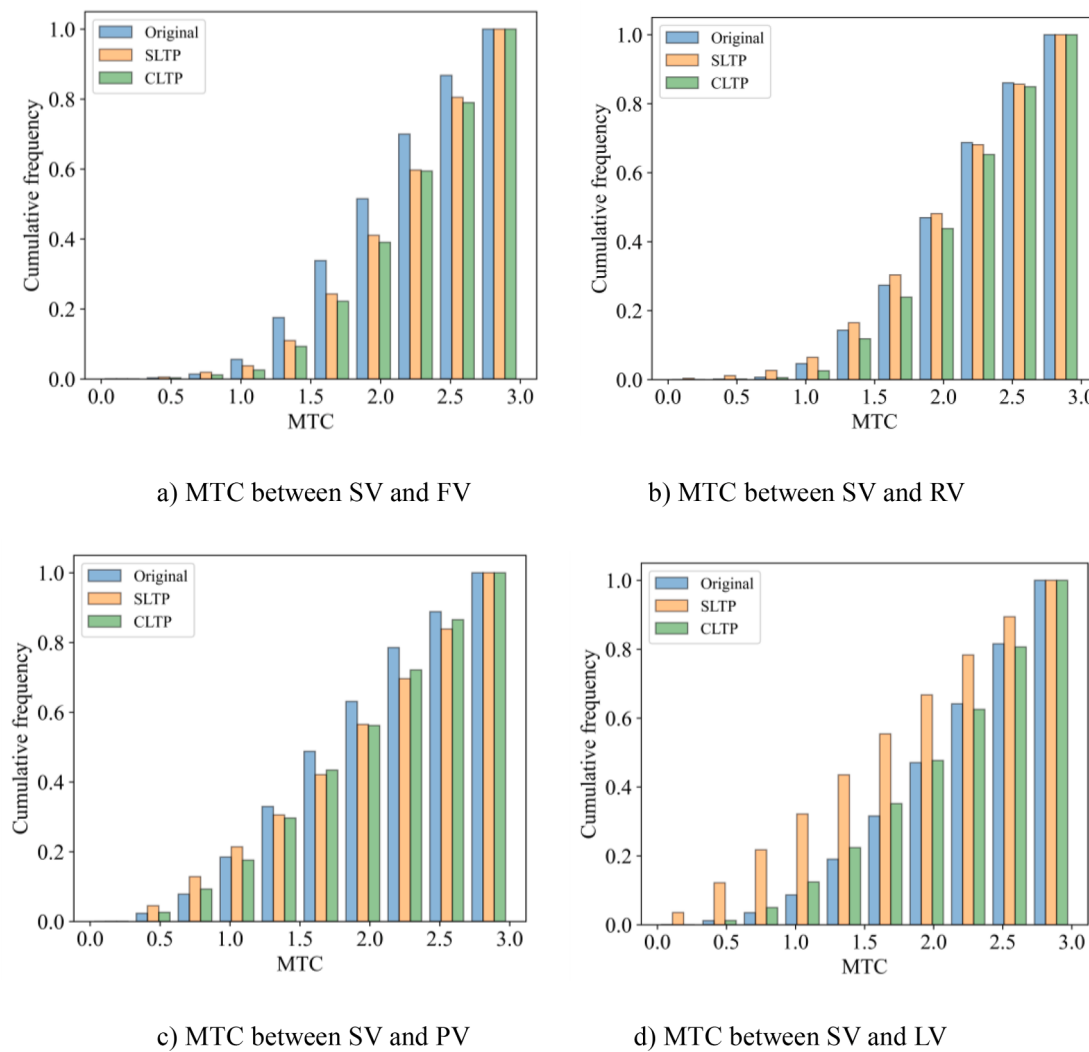


Fig. 15. Distribution of MTC between the SV and surrounding vehicles in all lane change samples.

To reflect the temporal risk of the LTP scheme given by three methods, the statistical results of TTC and TIT (Time Integrated Time-to-collision) are given in Table 3 and Table 4 during the lane changes. In Table 3 and Table 4, the average TTC between the SV and surrounding vehicles shows a significant increase, while the average TIT given by the CLTP reduces by 20.51 % and 62.37 % compared with the original and SLTP methods. The experimental results indicate that the CLTP model can successfully reduce the temporal risk between the SV and surrounding vehicles during a lane change.

The cumulative frequency diagrams of TTC between the SV and FV, RV, PV and LV for different methods are given in Fig. 13. The TTC of the CLTP shows a growing trend as a whole. Compared with the original method, the proportion of TTCs ($TTC < 5.5$ s) in CLTP between the SV and FV, RV, PV and LV decreased by 92.36 %, 45.07 %, 100 % and 88.58 % respectively, while that of the SLTP tends to go up. According to previous research results (Itoh and Inagaki, 2014; Lee et al., 2004; Young et al., 1995), when TTC is less than 5.5 s, it can be regarded as a traffic conflict. Thus, the finding proved that the CLTP model can effectively reduce the frequency of traffic conflicts caused by improper lane-changing behavior.

To demonstrate the spatial risk of the LTP scheme given by three methods, the statistical results of SDIs and MTCs (Margin to Collision) are given in Table 5 and Table 6 during the lane changes. Table 5 and Table 6 show that the average SDI and MTC of the CLTP method tend to go up, which can effectively reduce the spatial risk between the SV and

surrounding vehicles during the lane change. Compared with the original method, the average SDI in CLTP between the SV and FV, RV, PV and LV increases by 17.76 %, 6.95 %, 37.49 % and 13.72 %, while the average MTC in CLTP rises to 17.76 %, 2.55 %, 8.26 % and 19.49 % respectively.

Fig. 14 and Fig. 15 show that the statistical results of SDI and MTC of different methods between the SV and surrounding vehicles. If $SDI < 0$ or $MTC < 1$, the lane change process of the SV tends to be unsafe. From Fig. 14 and Fig. 15, it is observed that the unsafe space headways ($SDI < 0$ or $MTC < 1$) in CLTP between the SV and surrounding vehicles present a downward trend as a whole. Specifically, compared with the original method, the proportion of SDI ($SDI < 0$) between the SV and FV, RV, PV and LV has decreased by 98.78 %, -2%, 51.1 % and 43.61 % respectively. It is worth noting that the SDI between the SV and RV are almost higher than 0, which leads to insignificant trajectory optimization in CLTP. The findings proved that the CLTP model performed better optimization effect than the original and SLTP methods in terms of spatial risk reduction, which could help the SV keep safer distances from surrounding vehicles during a lane change.

5. Conclusions

Mature automatic driving technology can significantly improve traffic operation efficiency and traffic safety, which has attracted extensive attention in recent years. This study mainly focuses on the

lane-changing trajectory planning algorithm of AVs, which is the basis of lane change control in automatic driving systems. The existing research have achieved encouraging results in lane-changing trajectory planning for AVs, but there are still some defects to be solved. Some dynamic LTP models have considered the real-time traffic state of surrounding vehicles without investigating the predictability of the future motion information. Besides, few studies focus on an instantaneous risk identification method that integrates the temporal and spatial risk factors of the vehicle into the trajectory planning steps to pursue higher safety in a lane change. Therefore, this paper offers a co-evolutionary lane-changing trajectory planning method for AVs based on the instantaneous risk identification, which can improve the safety level of a lane change. Furthermore, high-resolution trajectory data of the HighD dataset from Germany are utilized to verify the effectiveness of the proposed model. The following conclusions are drawn in the paper.

- (1). GRU is adopted to predict the motion trajectory information of surrounding vehicles, and achieves satisfactory performance in capturing the future motion characteristics of vehicles.
- (2). Taking the safe interaction between the SV and surrounding vehicles into account, the proposed model can better monitor whether the current traffic environment meets the safety requirements of a lane change in real-time and quantify the temporal and spatial risks of the SV.
- (3). The proposed model is dedicated to minimizing the temporal and spatial risks, which can effectively reduce the frequency of traffic conflicts, improving the active safety performance of the lane-changing vehicles.

In this study, it is assumed that the surrounding vehicles always keep a car-following status in the two-lane scenario, and the proposed model is verified based on the driving data of the straight-line section on the highway, so the application scenarios are limited. In addition, the proposed model simply adopts the GRU algorithm to predict the vehicle trajectory, which leaves much room for further improvement. Therefore, more vehicle trajectory data are about to be collected to verify the proposed model in future work, exploring the intelligent algorithms with better performance to improve the prediction accuracy. Furthermore, the application scenarios of the model will be further explored to address the trajectory planning problems for a collaborative lane change, continuous lane changing, curve driving and other complex scenarios.

CRediT authorship contribution statement

Jiabin Wu: Conceptualization, Writing – original draft, Methodology. **Xiaohua Chen:** Software, Validation. **Yiming Bie:** Supervision, Writing – review & editing. **Wei Zhou:** Investigation.

Declaration of Competing Interest

The authors declare that they have no known competing financial interests or personal relationships that could have appeared to influence the work reported in this paper.

Data availability

Data will be made available on request.

Acknowledgment

This research is supported by the National Natural Science Foundation of China under grant number 71771062.

References

- Ali, Y., Zheng, Z., Haque, M.M., 2021. Modelling lane-changing execution behaviour in a connected environment: A grouped random parameters with heterogeneity-in-means approach. *Communications in Transportation Research* 1, 100009. <https://doi.org/10.1016/j.commr.2021.100009>.
- Bohren, J., Foote, T., Keller, J., Kushleyev, A., Lee, D., Stewart, A., Vernaza, P., Derenick, J., Spletzer, J., Satterfield, B., 2008. Little ben: The ben franklin racing team's entry in the 2007 DARPA urban challenge. *J. Field Robot.* 25 (9), 598–614. <https://doi.org/10.1002/rob.20260>.
- Chen, T., Shi, X., Wong, Y.D., et al., 2020. Predicting lane-changing risk level based on vehicles' space-series features: A pre-emptive learning approach. *Transp. Res. Part C: Emerg. Technol.* 116, 102646. <https://doi.org/10.1016/j.trc.2020.102646>.
- Chen, T., Wong, Y.D., Shi, X., et al., 2021. A data-driven feature learning approach based on Copula-Bayesian Network and its application in comparative investigation on risky lane-changing and car-following maneuvers. *Accid. Anal. Prev.* 154, 106061. <https://doi.org/10.1016/j.aap.2021.106061>.
- Dijkstra, E.W., 1959. A note on two problems in connexion with graphs. *Numer. Math.* 1 (1), 269–271. <https://doi.org/10.1007/BF01386390>.
- Duchoň, F., Babinec, A., Kajan, M., Beno, P., Florek, M., Fico, T., Jurišica, L., 2014. Path planning with modified a star algorithm for a mobile robot. *Procedia Eng.* 96, 59–69. <https://doi.org/10.1016/j.proeng.2014.12.098>.
- Fukuoka, Y., Hoshi, K., Kurosawa, R., 2013. Negotiating uneven terrain with a compliant designed unmanned ground vehicle equipped with locomotive master-slave operation. *J. Field Robot.* 30 (3), 349–370. <https://doi.org/10.1002/rob.21449>.
- Fukuyama, S., 2020. Dynamic game-based approach for optimizing merging vehicle trajectories using time-expanded decision diagram. *Transp. Res. Part C: Emerg. Technol.* 120, 102766. <https://doi.org/10.1016/j.trc.2020.102766>.
- Gardoni, P., 2017. Risk and reliability analysis, Risk and Reliability Analysis: Theory and Applications. Springer, pp. 3–24. 10.1007/978-3-319-52425-2.
- Gan, N., Zhang, M., Zhou, B., Chai, T., Wu, X., Bian, Y., 2022. Spatio-temporal heuristic method: a trajectory planning for automatic parking considering obstacle behavior. *Journal of Intelligent and Connected Vehicles* 5 (3), 177–187. <https://doi.org/10.1108/JICV-07-2022-0002>.
- Huang, J., Ji, Z., Peng, X., Hu, L., 2019. Driving Style Adaptive Lane-changing Trajectory Planning and Control. *China Journal of Highway and Transport* 32 (6), 226–239. <https://doi.org/10.19721/j.cnki.1001-7372.2019.06.023>.
- Itoh, M., Inagaki, T., 2014. Design and evaluation of steering protection for avoiding collisions during a lane change. *Ergonomics* 57 (3), 361–373. <https://doi.org/10.1080/00140139.2013.848474>.
- Jie, J., Zhi-rong, T., Ming-Yang, W., Jing-cheng, F., 2018. Path planning and tracking for lane changing based on model predictive control. *China J. Highway Transport.* 31 (4), 172. 10.19721/j.cnki.1001-7372.2018.04.021.
- Karimi, M., Roncoli, C., Alecsandru, C., et al., 2020. Cooperative merging control via trajectory optimization in mixed vehicular traffic. *Transp. Res. Part C: Emerg. Technol.* 116, 102663. <https://doi.org/10.1016/j.trc.2020.102663>.
- Khatib, O., 1986. Real-time obstacle avoidance for manipulators and mobile robots, Autonomous robot vehicles. Springer, pp. 396–404. 10.1007/978-1-4613-8997-2_29.
- Krajewski, R., Bock, J., Kloeker, L., Eckstein, L., 2018. The highd dataset: A drone dataset of naturalistic vehicle trajectories on german highways for validation of highly automated driving systems. In: 2018 21st International Conference on Intelligent Transportation Systems (ITSC), pp. 2118–2125. <https://doi.org/10.1109/ITSC.2018.8569552>.
- Lee, S.E., Olsen, E.C., Wierwille, W.W., 2004. A Comprehensive Examination of Naturalistic Lane-Changes. National Highway Traffic Safety Administration, United States <https://rosap.ntl.bts.gov/view/dot/4191>.
- Li, L., Gan, J., Zhou, K., et al., 2020. A novel lane-changing model of connected and automated vehicles: using the safety potential field theory. *Phys. A* 559, 1–14. <https://doi.org/10.1016/j.physa.2020.125039>.
- Lim, Q., Lim, Y., Muhammad, H., Tan, D.W.M., Tan, U.-X., 2021. Forward collision warning system for motorcyclists using smart phone sensors based on time-to-collision and trajectory prediction. *Journal of Intelligent and Connected Vehicles* 4 (3), 93–103. <https://doi.org/10.1108/jicv-11-2020-0014>.
- Liu, Z., Wang, Y., Wu, X., Zhang, C., NI, J., 2019. Collision Avoidance by Lane Changing Based on Linear Path-following Control. *China Journal of Highway and Transport* 32 (6), 86–95. <https://doi.org/10.19721/j.cnki.1001-7372.2019.06.009>.
- Luo, Y., Xiang, Y., Cao, K., Li, K., 2016. A dynamic automated lane change maneuver based on vehicle-to-vehicle communication. *Transp. Res. Part C: Emerg. Technol.* 62, 87–102. <https://doi.org/10.1016/j.trc.2015.11.011>.
- Ma, C., Yu, C., Yang, X., 2021. Trajectory planning for connected and automated vehicles at isolated signalized intersections under mixed traffic environment. *Transp. Res. Part C: Emerg. Technol.* 130, 103309. <https://doi.org/10.1016/j.trc.2021.103309>.
- McNaughton, M., Urmson, C., Dolan, J.M., Lee, J.-W., 2011. Motion planning for autonomous driving with a conformal spatiotemporal lattice. In: 2011 IEEE International Conference on Robotics and Automation, Shanghai, China, pp. 4889–4895. 10.1109/ICRA.2011.5980223.
- Mehrdad, T., Ramin, N., Ali, H., 2022. Distributed cooperative trajectory and lane changing optimization of connected automated vehicles: Freeway segments with lane drop. *Transp. Res. Part C: Emerg. Technol.* 143, 103761. <https://doi.org/10.1016/j.trc.2022.103761>.
- Nelson, W., 1989. Continuous-curvature paths for autonomous vehicles, Proceedings. In: 1989 International Conference on Robotics and Automation, pp. 1260–1264. <https://doi.org/10.1109/ROBOT.1989.100153>.
- Papadimitriou, I., Tomizuka, M., 2003. Fast lane changing computations using polynomials. In: Proceedings of the 2003 American Control Conference, 2003, Denver, CO, USA, pp. 48–53. 10.1109/ACC.2003.1238912.

- Sun, Z., Fang, S., 2017. Vehicle motion pattern analysis method for traffic conflict discrimination. *J. Tongji Univ. (Natural Science)* 45 (6), 839–846. <https://doi.org/10.11908/j.issn.0253-374x.2017.06.008>.
- Vadakkepat, P., Lee, T.H., Xin, L., 2001. Application of evolutionary artificial potential field in robot soccer system. In: Proceedings Joint 9th IFSA World Congress and 20th NAFIPS International Conference (Cat. No. 01TH8569), Vancouver, BC, Canada, pp. 2781-2785. Doi: 10.1109/NAFIPS.2001.943666.
- Wang, B., Gao, L., Juan, Z., 2018. Analysis of lane changing conflict based on TTA in expressway weaving area. *J. Syst. Simul.*, 30(9), 3306. 10.16182/j.issn1004731x.joss.201809010.
- Wang, Y., Wei, C., Ma, L., 2021. Dynamic Lane changing Trajectory Planning Model for Intelligent Vehicle Based on Quadratic Programming. *China Journal of Highway and Transport* 34 (7), 79–94. <https://doi.org/10.19721/j.cnki.1001-7372.2021.07.006>.
- Wu, J., Wen, H., Qi, W., 2020. A new method of temporal and spatial risk estimation for lane change considering conventional recognition defects. *Accid. Anal. Prev* 148, 105796. <https://doi.org/10.1016/j.aap.2020.105796>.
- Xu, L., Yin, G., Li, G., Bian, C., 2018. Stable trajectory planning and energy-efficiency control allocation of lane change maneuver for autonomous electric vehicle. *Journal of Intelligent and Connected Vehicles* 1 (2), 55–65. <https://doi.org/10.1108/JICV-12-2017-0002>.
- Yang, C., Chen, X., Lin, X., et al., 2022. Coordinated trajectory planning for lane-changing in the weaving areas of dedicated lanes for connected and automated vehicles. *Transp. Res. Part C: Emerg. Technol* 144, 103864. <https://doi.org/10.1016/j.trc.2022.103864>.
- Yang, D., Zheng, S., Wen, C., Jin, P.J., Ran, B., 2018. A dynamic lane-changing trajectory planning model for automated vehicles. *Transp. Res. Part C: Emerg. Technol*, 95, 228-247. 10.1016/j.trc.2018.06.007.
- Yang, G., Zhang, D.-H., Li, K.-Q., Luo, Y., 2017. Cooperative same-direction automated lane-changing based on vehicle-to-vehicle communication. *J. Highway Transport. Res. Develop.* 34 (1), 120–129. <https://oversea.cnki.net/kcms/detail/detail.aspx?dbcode=CJFD&dbname=CJFD2017&filename=GLJK201701018>.
- Yao, H., Li, X., 2021. Lane-change-aware connected automated vehicle trajectory optimization at a signalized intersection with multi-lane roads. *Transp. Res. Part C: Emerg. Technol* 129, 103182. <https://doi.org/10.1016/j.trc.2021.103182>.
- Yao, W., Zeng, Q., Lin, Y., Xu, D., Zhao, H., Guillemand, F., Geronimi, S., Aioun, F., 2016. On-road vehicle trajectory collection and scene-based lane change analysis: Part II. *IEEE trans. Intell. Transp. Syst.* 18 (1), 206–220. <https://doi.org/10.1109/TITS.2016.2571724>.
- Young, S.K., Eberhard, C.A., Moffa, P.J., 1995. Development of performance specifications for collision avoidance systems for lane change, merging, and backing. Task 2 interim report: Functional goals establishment. US Department of Transportation, National Highway Traffic Safety Administration. <https://rosap.ntl.bts.gov/view/dot/3066>.
- Yu Bai, Yu Zhang & Jia Hu., 2021. A motion planner enabling cooperative lane changing: Reducing congestion under partially connected and automated environment. *J. Intelligent Transport. Syst.*, 25, 5: 469-481. 10.1080/15472450.2020.1820332.
- Zeng, D., Yu, Z., Xiong, L., Zhao, J., Zhang, P., Li, Z., Fu, Z., Yao, J., Zhou, Y., 2019. A novel robust lane change trajectory planning method for autonomous vehicle. In: 2019 IEEE Intelligent Vehicles Symposium (IV), Paris, France, pp. 486-493. 10.1109/IVS.2019.8814151.
- Zhang, S., Deng, W., Zhao, Q., Sun, H., Litkouhi, B., 2013. Dynamic trajectory planning for vehicle autonomous driving. In: 2013 IEEE International Conference on Systems, Man, and Cybernetics, Manchester, UK, pp. 4161-4166. 10.1109/SMC.2013.709.
- Zhang, S., Deng, W., Zhao, Q., Sun, H., Litkouhi, B., 2012. An intelligent driver model with trajectory planning. In: 2012 15th International IEEE conference on intelligent transportation systems, Anchorage, AK, USA, pp. 876-881. 10.1109/ITSC.2012.6338651.
- Zhai, C., Wu, W., 2021. Designing continuous delay feedback control for lattice hydrodynamic model under cyber-attacks and connected vehicle environment. *Commun. Nonlinear Sci. Numer. Simul.* 95, 105667 <https://doi.org/10.1016/j.apm.2022.04.010>.
- Zhai, C., Wu, W., 2022. A continuum model considering the uncertain velocity of preceding vehicles on gradient highways. *Physica A* 558, 126561. <https://doi.org/10.1016/j.physa.2021.126561>.
- Zhai, C., Wu, W., Xiao, Y., 2022. Cooperative car-following control with electronic throttle and perceived headway errors on gyroidal roads. *Appl. Math. Model.* 108, 770–786. <https://doi.org/10.1016/j.apm.2022.04.010>.
- Ziegler, J., Stiller, C., 2009. Spatiotemporal state lattices for fast trajectory planning in dynamic on-road driving scenarios. In: 2009 IEEE/RSJ International Conference on Intelligent Robots and Systems, pp. 1879–1884. <https://doi.org/10.1109/IROS.2009.5354448>.